


# In-phase and out-of-phase spin pumping effects in Py/Ru/Py synthetic antiferromagnetic structures

Zhaocong Huang(黄兆聪), Xuejian Tang(唐学健), Qian Chen(陈倩), Wei Jiang(蒋伟), Qingjie Guo(郭庆杰), Milad Jalali, Jun Du(杜军), and Ya Zhai(翟亚)

**Citation:**Chin. Phys. B, 2024, 33 (**9**): 097202. DOI: 10.1088/1674-1056/ad553d
Journal homepage: http://cpb.iphy.ac.cn; http://iopscience.iop.org/cpb

**What follows is a list of articles you may be interested in**

---

## Spin transport characteristics modulated by the GeBi interlayer in $Y_3Fe_5O_{12}$/GeBi/Pt heterostructures

Mingming Li(李明明), Lei Zhang(张磊), Lichuan Jin(金立川), and Haizhong Guo(郭海中)
Chin. Phys. B, 2024, 33 (**2**): 027201. DOI: 10.1088/1674-1056/ace3aa

## Inverse spin Hall effect in ITO/YIG exited by spin pumping and spin Seebeck experiments

Kejian Zhu(朱科建), Weijian Lin(林伟坚), Yangtao Su(苏仰涛), Haibin Shi(石海滨), Yang Meng(孟洋), Hongwu Zhao(赵宏武)
Chin. Phys. B, 2019, 28 (**1**): 017201. DOI: 10.1088/1674-1056/28/1/017201

## Spin depolarization dynamics of $WSe_2$ bilayer

Binghui Niu(牛秉慧), Jialiang Ye(叶加良), Ting Li(李婷), Ying Li(李莹), Xinhui Zhang(张新惠)
Chin. Phys. B, 2018, 27 (**5**): 057202. DOI: 10.1088/1674-1056/27/5/057202

## The origin of spin current in YIG/nonmagnetic metal multilayers at ferromagnetic resonance

Yun Kang(康韵), Hai Zhong(钟海), Runrun Hao(郝润润), Shujun Hu(胡树军), Shishou Kang(康仕寿), Guolei Liu(刘国磊), Yin Zhang(张引), Xiangrong Wang(王向荣), Shishen Yan(颜世申), Yong Wu(吴勇), Shuyun Yu(于淑云), Guangbing Han(韩广兵), Yong Jiang(姜勇), Liangmo Mei(梅良模)
Chin. Phys. B, 2017, 26 (**4**): 047202. DOI: 10.1088/1674-1056/26/4/047202

## Spin pumping through magnetic impurity effect

Deng Wei-Yin (邓伟胤), Sheng Li (盛利), Xing Ding-Yu (邢定钰)
Chin. Phys. B, 2015, 24 (**8**): 087202. DOI: 10.1088/1674-1056/24/8/087202

---

# In-phase and out-of-phase spin pumping effects in Py/Ru/Py synthetic antiferromagnetic structures

Zhaocong Huang(黄兆聪)[1,†], Xuejian Tang(唐学健)[1,†], Qian Chen(陈倩)[1,‡], Wei Jiang(蒋伟)[1], Qingjie Guo(郭庆杰)[1], Milad Jalali[1], Jun Du(杜军)[2], and Ya Zhai(翟亚)[1,§]

[1] *Key Laboratory of Quantum Materials and Devices of Ministry of Education, School of Physics, Southeast University, Nanjing* 211189, *China*
[2] *National Laboratory of Solid Microstructures, Nanjing University, Nanjing* 210093, *China*

(Received 2 June 2024; revised manuscript received 5 June 2024; accepted manuscript online 7 June 2024)

The spin pumping effect in magnetic heterostructures and multilayers is a highly effective method for the generation and transmission of spin currents. In the increasingly prominent synthetic antiferromagnetic structures, the two ferromagnetic layers demonstrate in-phase and out-of-phase states, corresponding to acoustic and optical precession modes. Within this context, our study explores the spin pumping effect in Py/Ru/Py synthetic antiferromagnetic structures across different modes. The heightened magnetic damping resulting from the spin pumping effect in the in-phase state initially decreases with increasing Py thickness before stabilizing. Conversely, in the out-of-phase state, the amplified damping exceeds that of the in-phase state, suggesting a greater spin relaxation within this configuration, which demonstrates sensitivity to alterations in static exchange interactions. These findings contribute to advancing the application of synthetic antiferromagnetic structures in magnonic devices.

**Keywords:** spin pumping, spin transmission, synthetic antiferromagnetic structures , spin dynamics

**PACS:** 72.25.Pn, 72.25.Mk, 76.50.+g, 67.30.hj **DOI:** 10.1088/1674-1056/ad553d

## 1. Introduction

Synthetic antiferromagnetic (SAF) structures have recently garnered significant attention due to their low stray fields, high thermal stability, and high intrinsic frequencies, which are key factors in enhancing magnetic storage density and operational speeds.[1–3] Consisting of two ferromagnetic layers (FM) coupled antiferromagnetically through a nonmagnetic spacer (NM), SAFs are characterized by complex magnetodynamics processes involving spin pumping at the FM/NM interface,[4–6] spin transmission in the NM,[7–9] and interlayer dynamic coupling between the two FMs.[2,10,11]

The magnetic states of the two FM layers in a magnetic trilayer structure play a crucial role in determining the spin current transmission and dynamic coupling within the system. Based on the different magnetic ground states, parallel and antiparallel FMs, magnon valves[12,13] and magnon junctions[14] with different spin transmission properties have been developed. In the magnetic excited state, acoustic and optical modes can be achieved, depending on the phase difference in the precession of the two FM layers.[15–20] The pumped spin current and the associated spin transmission and dynamic coupling effects differ under different precession states. Prior research has established that the dynamic characteristics of these precession modes can be influenced by the thickness of the spacer layer[21] and the spin–orbit torque within the system.[22] Besides, the Gilbert damping of both modes have been theoretically elucidated in relation to the dynamic exchange coupling induced by the spin current.[23] Nevertheless, experimental investigations of spin pumping effects in the in-phase and out-of-phase precession states within SAF structures with varying thicknesses of the ferromagnetic layers are demanded.

In this study, we explore the spin pumping effects in Py/Ru/Py synthetic antiferromagnetic structures under both in-phase and out-of-phase spin precession states. Through ferromagnetic resonance experiments, we investigate the spin relaxation processes under different precession modes. By considering the variations in the thickness of the ferromagnetic layers and the interlayer static magnetic exchange interactions, we reveal that the spin current pumped from the out-of-phase spin precession state experiences more pronounced spin relaxation and shows greater sensitivity to changes in static exchange interactions. This study contributes to the understanding of the potential applications of SAF structures in magnonic devices.

## 2. Experiments

The primary structure of our samples consists of Py($d$)/Ru(0.5)/Py($d$) with all thicknesses specified in nanometers. Additionally, a series of Py(5)/Ru($d_{\mathrm{Ru}}$) samples are prepared for comparison. These samples are deposited onto silicon dioxide (Si/$SiO_2$) substrates using magnetron sputtering with a 3-nm tantalum (Ta) buffer layer. To prevent oxidation,

[†]These authors contributed equally to this work.
[‡]Corresponding author. E-mail: qchen2022@seu.edu.cn
[§]Corresponding author. E-mail: yazhai@seu.edu.cn

© 2024 Chinese Physical Society and IOP Publishing Ltd 

a protective 2-nm Al cap is applied in situ to all films. Prior to the sputtering process, the base pressure is maintained below $7.5\times10^{-8}$ Torr (1 Torr = $1.33322\times10^{2}$ Pa). The argon working pressure is carefully set at 2.25 mTorr with a 30-sccm gas flow during deposition, while the deposition powers for Py and Ru are controlled at 20 W and 5 W, respectively. To ensure the quality of the films, x-ray diffraction (XRD) characterization is carried out on the Py and Ru films individually, as shown in Fig. 1(a). The observation of Py (111) diffraction peaks and Ru (002) and (101) diffraction peaks indicates that the prepared Py and Ru films are in a polycrystalline state. To accurately control the thickness of the Py and Ru films, x-ray reflectometry (XRR) testing is conducted on the Py and Ru films. Based on the XRR results shown in Fig. 1(b) and the sputtering time, the sputtering rates for Py and Ru are determined separately to be 0.95 Å/s and 0.16 Å/s.

The static and dynamic magnetic properties of the samples are characterized using a vibrating sample magnetometer (VSM) and a vector network analyzer ferromagnetic resonance (VNA-FMR), respectively. During VNA-FMR measurements, the samples are placed face down on a coplanar waveguide and subjected to a microwave field $h$. The power of $h$ is maintained at 0 dBm, and an external magnetic field $H$ is applied perpendicular to $h$. The microwave signal $S_{21}$ transmission is measured at different fixed magnetic fields $H$ while sweeping the frequency from 1 GHz to 20 GHz. By extracting the $S_{21}$ signal at different $H$ and a specific frequency, we are able to obtain the field-sweeping spectrum of FMR. All measurements are conducted at room temperature.

## 3. Results and discussion

Figure 1(c) shows the hysteresis loops obtained from VSM measurements of a single layer Py film, with the magnetic field parallel to the in-plane easy and hard axes of magnetization. The sample exhibits a uniaxial magnetic anisotropy in the film plan. The saturation magnetization is about 1200 emu/cm$^3$ and the coercivity is close to 4 Oe (1 Oe = 79.5775 A·m$^{-1}$), demonstrating excellent soft magnetic properties.

To determine the spin diffusion length[24] $\lambda_{\mathrm{Ru}}$ of Ru and the spin mixing conductance[25–27] $g_{\mathrm{eff}}^{\uparrow\downarrow}$ at the Py/Ru interface, we carry out FMR measurements on Py/Ru samples. These two factors ($g_{\mathrm{eff}}^{\uparrow\downarrow}$ and $\lambda_{\mathrm{Ru}}$) are crucial for our subsequent study of dynamic coupling in the Py/Ru/Py structures. Field-sweeping FMR spectra of Py(5)/Ru(0.5) are depicted in Fig. 1(c), which can be fitted by symmetric and antisymmetric Lorentzian lineshapes[28]

$$S_{21}=\frac{K_1\Delta H^2+K_2\Delta H\,(H-H_{\mathrm{res}})}{\Delta H^2+4\,(H-H_{\mathrm{res}})^2},$$

where $H_{\mathrm{res}}$ is the resonance field, $\Delta H$ is the linewidth of the FMR spectrum, $K_1$ and $K_2$ are the coefficients of the symmetric and antisymmetric Lorentzian components respectively. By examining the frequency dependence of $\Delta H$, as shown in Fig. 1(d), we extract the magnetodynamic damping $\alpha$ of the sample according to[28]

$$\Delta H=\Delta H_0+\frac{4\pi\alpha}{\gamma}f, \tag{1}$$

where $\Delta H_0$ is the inhomogeneous broadening, and $\gamma=g\mu_{\mathrm{B}}/\hbar$ is the gyromagnetic ratio ($g$ is the Lande factor and $\mu_{\mathrm{B}}$ is the Bohr magneton). The deduced relationship between the damping factor and the thickness of Ru in Py/Ru structure is illustrated in Fig. 1(e). According to the conventional spin-pumping model, the incremental damping induced by spin pumping can be expressed as[25,29,30]

$$\Delta\alpha=\frac{g\mu_{\mathrm{B}}g_{\mathrm{eff}}^{\uparrow\downarrow}}{4\pi M_{\mathrm{s}}d}\left[1-\exp\left(\frac{-2d_{\mathrm{Ru}}}{\lambda_{\mathrm{Ru}}}\right)\right]. \tag{2}$$

Through fitting, we determine the spin mixing conductance $g_{\mathrm{eff}}^{\uparrow\downarrow}$ at Py/Ru interface to be $1.15\times10^{15}$ cm$^{-2}$, and the spin diffusion length $\lambda_{\mathrm{Ru}}$ in Ru is found to be $8.68\pm2.08$ nm. Hence, by opting for a 0.5-nm thickness of Ru spacer in constructing the Py/Ru/Py structure, the spin current can seamlessly traverse from one Py film through the Ru spacer to the adjacent Py layer, enabling the establishment of dynamic coupling interactions.

After delineating the spin pumping process at the Py/Ru interface, we conduct further investigations into spin pumping effect in Py/Ru/Py synthetic antiferromagnetic structures. First, we analyze the spin dynamics modes in samples with different thicknesses $d$ of Py. Figures 2(a)–2(c) depict the FMR results at different frequencies and magnetic fields obtained from frequency-sweep FMR measurement, with colors representing the microwave transmission signal $S_{21}$. From these results, we clearly distinguish at least two distinct collective excitation modes of the magnetic moments, specifically the acoustic mode (AM) and optical mode (OM). Here, the AM signifies the in-phase motion of the two Py layers, while the OM denotes the out-of-phase motion.[16,18] The acoustic and optical modes are discerned based on their respective resonance positions. Typically, the resonance field of the acoustic mode across different frequencies is close to the Kittel mode of the Py/Ru, as depicted in Fig. 1(d), while the resonance field of the optical mode is different.[31] Hence, we infer that in the acquired frequency-sweep FMR spectra (Figs. 2(a)–(c)), modes positioned at higher frequencies correspond to acoustic modes, while those at lower frequencies correspond to optical modes, which are depicted by green circles and yellow pentagons, respectively. Moreover, upon reaching a Py thickness of 30 nm, in addition to the AM and OM modes, an extra excitation mode at higher frequencies is observed, as highlighted by the blue triangles in Fig. 2(c), corresponding to the first-order perpendicular standing spin wave (PSSW) mode.

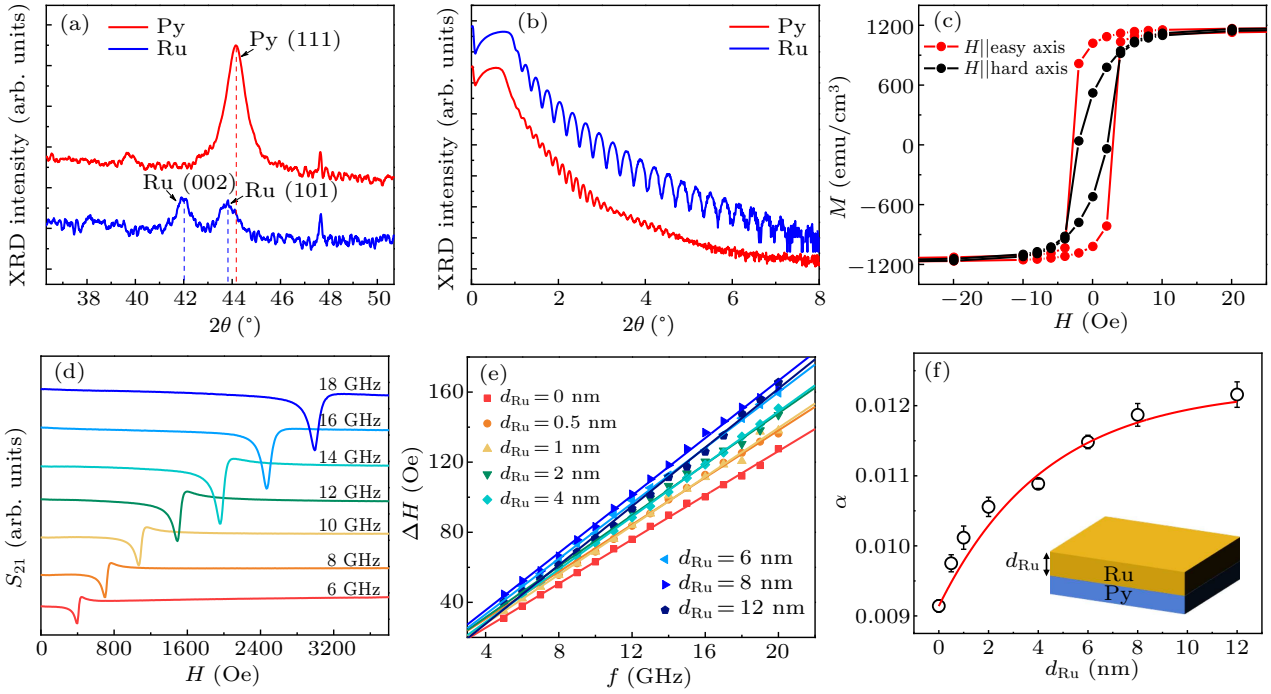



**Fig. 1.** (a) X-ray diffraction (XRD) spectra and (b) x-ray reflectometry (XRR) results of Py and Ru films. (c) In-plane hysteresis loops obtained from VSM measurements of Py film. (d) Field-sweeping FMR spectra of Py(5)/Ru(0.5) at different frequencies. (e) Frequency dependency of the FMR linewidth of Py(5)/Ru($d_{\mathrm{Ru}}$). (f) The deduced relationship between the damping factor and the thickness of Ru in Py(5)/Ru($d_{\mathrm{Ru}}$) structures.

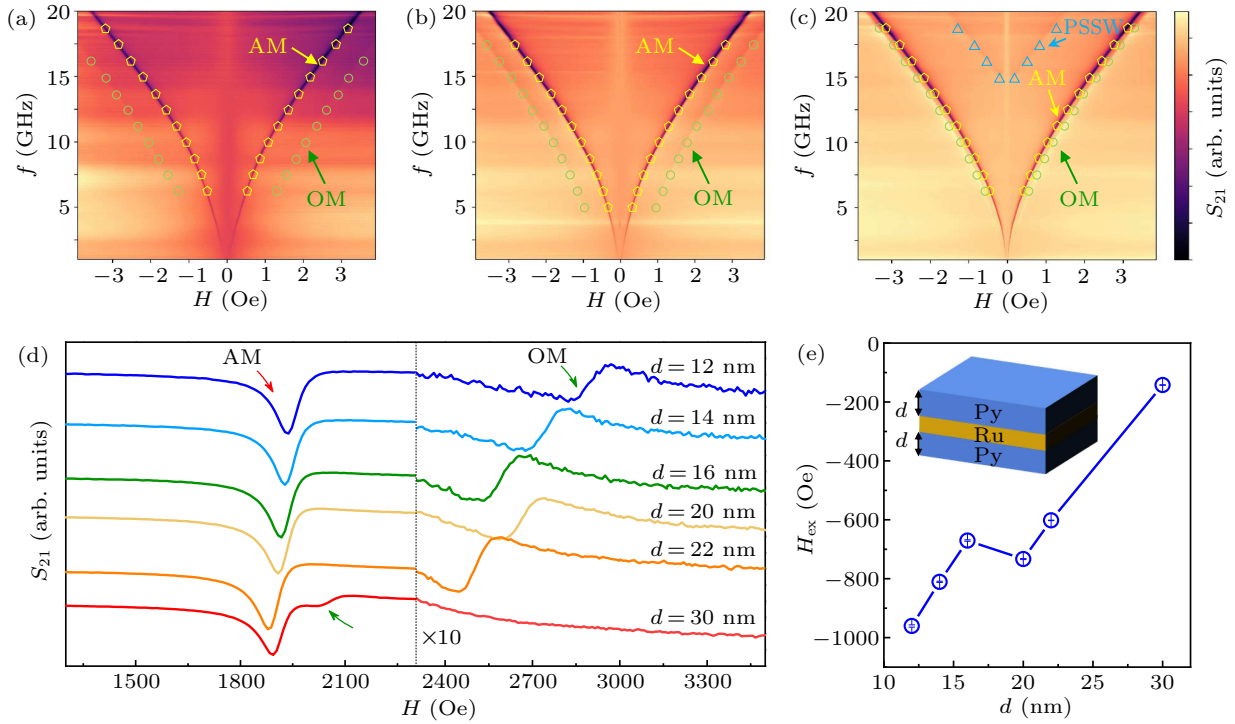



**Fig. 2.** (a) The FMR results at different frequencies and magnetic fields obtained from frequency-sweep FMR measurements on Py($d$)/Ru(0.5)/Py($d$) with (a) $d = 12$ nm, (b) $d = 20$ nm, (c) $d = 30$ nm. (d) The field-sweeping FMR spectra of Py($d$)/Ru(0.5)/Py($d$) with different $d$ at 14 GHz. The data on the right of the dashed line has been magnified tenfold on the vertical axis. (e) Variation of $H_{\mathrm{ex}}$ with increasing thickness of Py($d$)/Ru(0.5)/Py($d$) structures.

Figure 2(d) shows the field-sweeping ferromagnetic resonance spectra of Py($d$)/Ru(0.5)/Py($d$) with different $d$ at pressure 14 GHz. At the same frequency, the resonance field of the acoustic mode is consistently smaller than that of the optical mode, indicating a negative interlayer exchange coupling between the two Py layers.[16] The interlayer exchange coupling field, $H_{\mathrm{ex}}$, can be determined through the fitting of the following equations:[31]

$$\left(\frac{2\pi f^{\mathrm{AM}}}{\gamma}\right)^2 = \left(H_{\mathrm{r}}^{\mathrm{AM}}\right)\left(H_{\mathrm{r}}^{\mathrm{AM}} + 4\pi M_{\mathrm{eff}}\right),$$

$$\left(\frac{2\pi f^{\mathrm{OM}}}{\gamma}\right)^2 = \left(H_{\mathrm{r}}^{\mathrm{OM}} + H_{\mathrm{ex}}\right)\left(H_{\mathrm{r}}^{\mathrm{OM}} + H_{\mathrm{ex}} + 4\pi M_{\mathrm{eff}}\right),$$

where $f^{\mathrm{AM}}$ and $f^{\mathrm{OM}}$ represent the frequencies corresponding

to the resonance fields $H_r^{AM}$ and $H_r^{OM}$ of the acoustic and optical modes, respectively. Certainly, the value of $H_{ex}$ can also be approximated by the magnetic field difference between the resonance fields of the AM and OM modes at the same high frequency,[32] and the results are consistent. As illustrated in Fig. 2(e), with an increase in the Py thickness, the magnitude of $|H_{ex}|$ shows a decreasing trend, gradually approaching 0, and $H_{ex}$ remains negative within 30 nm. The negative $H_{ex}$ observed in this study confirms the synthetic antiferromagnetic structure of Py/Ru(0.5)/Py. According to the theory of the Ruderman–Kittel–Kasuya–Yosida (RKKY) interaction,[33–35] antiferromagnetic coupling only occurs within a limited range of nonmagnetic layer thickness. With the increase in the thickness of the ferromagnetic layer, the interlayer interactions experienced by the magnetic moments far from the Py/Ru interface may extend beyond the window of antiferromagnetic coupling, leading to a competition between direct exchange interaction and interlayer interaction. Therefore, in the context of antiferromagnetic coupling systems, the absolute value of the exchange interaction manifests a declining trend as the thickness of the ferromagnetic layer increases. However, it is worth noting that in the vicinity of a 20-nm ferromagnetic layer, there is a slight fluctuation in the variation of $H_{ex}$, which may be attributed to the competition between direct exchange interaction and RKKY interaction within the system.

Furthermore, we investigate the spin pumping effects at different precession states. Due to the spin pumping effects manifesting as the transfer of spin angular momentum, it directly impacts the magnitude of the magnetic damping factor of the ferromagnetic layer. In systems with significant spin pumping, the increment in magnetic damping is larger, and spin backflow may potentially lead to a decrease in magnetic damping. Therefore, we primarily focus on the resonance linewidth variations with frequency in the Py/Ru/Py structures with different Py thicknesses, concerning acoustic and optical modes, as illustrated in Figs. 3(a) and 3(b). It is observed that the linewidth of the magnetic moment FMR under the out-of-phase optical mode increases significantly with frequency compared to the in-phase acoustic mode. Due to the weaker signal of the optical mode, the linewidth obtained from fitting exhibits a larger error compared to the acoustic mode. The frequency dependency of the acoustic mode shows a pronounced linear variation. For the optical mode, the frequency dependence of the linewidth generally demonstrates a linear rising trend, as depicted in the shaded region of Fig. 3(b). While some data points deviate from linearity, we can still fit them using Eq. (1) to derive the magnetic damping factor with certain uncertainties, and analyze it within the error range. When the thickness of the ferromagnetic layer reaches 30 nm, the linewidth of the optical mode shows a clear linear increase with frequency. Moreover, as the thickness of the ferromagnetic layer increases, there is a slight decrease in the amplitude of the resonance linewidth variations with frequency.

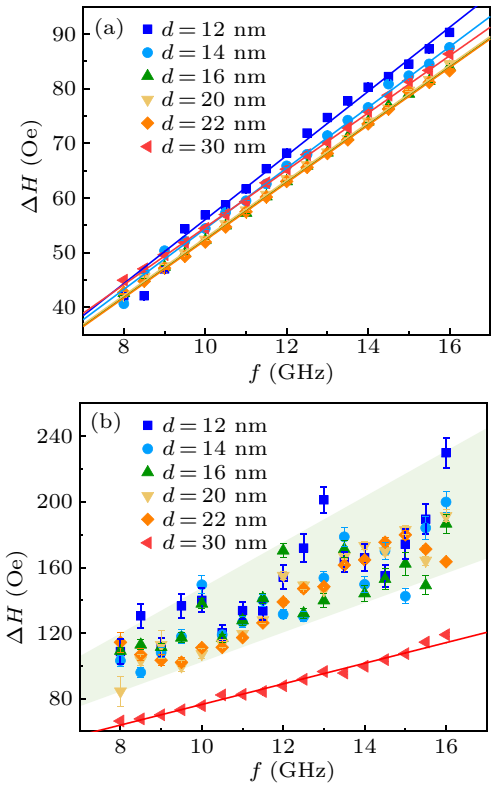



**Fig. 3.** Frequency dependency of the FMR linewidth of (a) in-phase (AM) and (b) out-of-phase (OM) states.

We fitted the frequency dependency of the resonance linewidth of the AM and OM using Eq. (1), with the results shown in Fig. 4 with a dual-$y$ axis representation. It is observed that the magnetic damping extracted from the out-of-phase state is generally higher than that extracted from the in-phase state, indicating more spin relaxations occur on the pumped spin currents from Py layers under the out-of-phase precession state.[29,30] When the Py thickness increases from 12 nm to 16 nm, the magnetic damping extracted from the in-phase state decreases from $0.0086 \pm 0.0002$ to $0.0078 \pm 0.0001$, while the magnetic damping extracted from the out-of-phase state decreases from $0.016 \pm 0.003$ to $0.011 \pm 0.002$. With further increase in Py thickness, the magnetic damping extracted from the in-phase state remains around 0.0078, while the magnetic damping extracted from the out-of-phase state initially increases, then gradually decreases after $d$ exceeds 20 nm. This fluctuation trend of the OM magnetic damping is similar to the fluctuation trend of Hex with $d$. Therefore, we speculate that static magnetic exchange interactions, encompassing the interplay between direct exchange interaction and RKKY interaction within the system, could impact dynamic coupling. The out-of-phase spin precession state seems to exhibit heightened sensitivity to this effect associated with dynamic coupling.

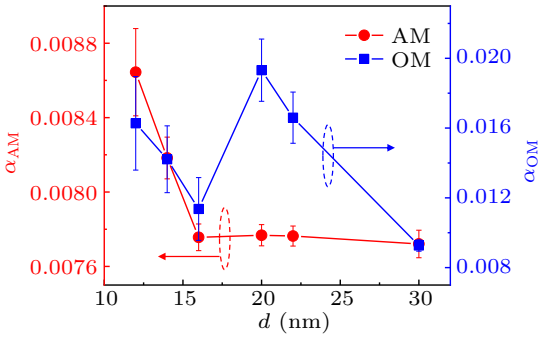



**Fig. 4.** Magnetic damping extracted from the in-phase (AM) and out-of-phase (OM) states as functions of the Py thickness in Py($d$)/Ru(0.5)/Py($d$) structures.

## 4. Conclusion

In conclusion, our study uncovers the spin pumping effect in Py/Ru/Py synthetic antiferromagnetic structures, delineating the influence of in-phase and out-of-phase spin precession states associated with the acoustic and optical modes, respectively. The determined spin mixing constant at the Py/Ru interface is $1.15 \times 10^{15}$ cm$^{-2}$, while a spin diffusion length of 8.68 nm is established in Py/Ru structures, showcasing the efficient transmission of spin currents and interlayer dynamic coupling facilitated by the 0.5-nm Ru spacer in the Py/Ru/Py structure. The negative $H_{ex}$ derived from FMR analysis confirms the synthetic antiferromagnetic characteristics of the Py/Ru(0.5)/Py structures and exhibits a diminishing trend with increasing Py thickness. Notably, our results indicate a higher magnetic damping in the out-of-phase state compared to the in-phase state, suggestive of the larger spin relaxation of the pumped spin currents from Py layers under the out-of-phase precession state. The variation behavior of magnetic damping with Py thickness in the out-of-phase state mirrors the trends observed in $H_{ex}$, implying a potential impact of interlayer static magnetic exchange interactions on dynamic coupling, particularly accentuated in the out-of-phase precession state. Our findings not only provide valuable insights into the dynamic behavior of synthetic antiferromagnetic structures, but also highlight their potential significance for the development of advanced magnonic devices.

## Acknowledgements

Project supported by National Key Research and Development Program of China (Grant No. 2023YFA1406603), the National Natural Science Foundation of China (Grant Nos. 52071079, 12274071, 12374112, and T2394473), and Jiangsu Funding Program for Excellent Postdoctoral Talent (Grant No. 2023ZB491).

## References

[1] Legrand W, Maccariello D, Ajejas F, Collin S, Vecchiola A, Bouzehouane K, Reyren N, Cros V and Fert A 2020 *Nat. Mater.* **19** 34
[2] Wang Y, Zhang Y, Li C, Wei J, He B, Xu H, Xia J, Luo X, Li J, Dong J, He W, Yan Z, Yang W, Ma F, Chai G, Yan P, Wan C, Han X and Yu G 2024 *Nat. Commun.* **15** 2077
[3] Yang S H, Ryu K S and Parkin S 2015 *Nat. Nanotech.* **10** 221
[4] Costache M V, Sladkov M, Watts S M, van der Wal C H and van Wees B J 2006 *Phys. Rev. Lett.* **97** 216603
[5] Mosendz O, Pearson J E, Fradin F Y, Bauer G E W, Bader S D and Hoffmann A 2010 *Phys. Rev. Lett.* **104** 046601
[6] Tserkovnyak Y, Brataas A and Bauer G E W 2002 *Phys. Rev. B* **66** 224403
[7] Chen Q, Ruan X, Yuan H, Zhou X, Kou Z, Huang Z, Xu Y and Zhai Y 2020 *Appl. Phys. Lett.* **116** 132403
[8] Kajiwara Y, Harii K, Takahashi S, Ohe J, Uchida K, Mizuguchi M, Umezawa H, Kawai H, Ando K, Takanashi K, Maekawa S and Saitoh E 2010 *Nature* **464** 262
[9] Fan Y, Finley J, Han J, Holtz M E, Quarterman P, Zhang P, Safi T S, Hou J T, Grutter A J and Liu L 2021 *Adv. Mater.* **33** 2008555
[10] Chen J, Liu C, Liu T, Xiao Y, Xia K, Bauer G E W, Wu M and Yu H 2018 *Phys. Rev. Lett.* **120** 217202
[11] Heinrich B, Tserkovnyak Y, Woltersdorf G, Brataas A, Urban R and Bauer G E W 2003 *Phys. Rev. Lett.* **90** 187601
[12] Guo C Y, Wan C H, Wang X, Fang C, Tang P, Kong W J, Zhao M K, Jiang L N, Tao B S, Yu G Q and Han X F 2018 *Phys. Rev. B* **98** 134426
[13] Wu H, Huang L, Fang C, Yang B S, Wan C H, Yu G Q, Feng J F, Wei H X and Han X F 2018 *Phys. Rev. Lett.* **120** 097205
[14] Guo C Y, Wan C H, He W Q, Zhao M K, Yan Z R, Xing Y W, Wang X, Tang P, Liu Y Z, Zhang S, Liu Y W and Han X F 2020 *Nat. Electron.* **3** 304
[15] Li Y, Zhang Z, Liu C, Zheng D, Fang B, Zhang C, Chen A, Ma Y, Wang C, Liu H, Shen K, Manchon A, Xiao J Q, Qiu Z, Hu C M and Zhang X 2024 *Nat. Commun.* **15** 2234
[16] Omelchenko P, Girt E and Heinrich B 2019 *Phys. Rev. B* **100** 144418
[17] Xie Z K, Cai J W, Cheng Z H and He W 2024 *Appl. Phys. Lett.* **124** 042406
[18] Zivieri R, Giovannini L and Nizzoli F 2000 *Phys. Rev. B* **62** 14950
[19] Sud A, Zollitsch C W, Kamimaki A, Dion T, Khan S, Iihama S, Mizukami S and Kurebayashi H 2020 *Phys. Rev. B* **102** 100403
[20] Tanaka K, Moriyama T, Nagata M, Seki T, Takanashi K, Takahashi S and Ono T 2014 *Appl. Phys. Express* **7** 063010
[21] Yang H, Li Y and Bailey W E 2016 *Appl. Phys. Lett.* **108** 242404
[22] Karube S, Hoshika T, Zhang C, Kohda M and Nitta J 2022 *Appl. Phys. Express* **15** 103001
[23] Kamimaki A, Iihama S, Taniguchi T and Mizukami S 2019 *Appl. Phys. Lett.* **115** 132402
[24] Zhang W, Vlaminck V, Pearson J E, Divan R, Bader S D and Hoffmann A 2013 *Appl. Phys. Lett.* **103** 242414
[25] Chen Q, Cao L, Li J, Fu Q, Zhu Y, Guo Q, Liu R, Li T, Zhang W, Du J, Zheng J, Huang Z, Wong P K J, Fang B, Zeng Z and Zhai Y 2022 *Appl. Phys. Lett.* **120** 242405
[26] Deorani P and Yang H 2013 *Appl. Phys. Lett.* **103** 232408
[27] Zhu L, Ralph D C and Buhrman R A 2019 *Phys. Rev. Lett.* **123** 057203
[28] Yin Y, Pan F, Ahlberg M, Ranjbar M, Dürrenfeld P, Houshang A, Haidar M, Bergqvist L, Zhai Y, Dumas R K, Delin A and Åkerman J 2015 *Phys. Rev. B* **92** 024427
[29] Shaw J M, Nembach H T and Silva T J 2012 *Phys. Rev. B* **85** 054412
[30] Tserkovnyak Y, Brataas A and Bauer G E W 2002 *Phys. Rev. Lett.* **88** 117601
[31] Wang W, Li P, Cao C, Liu F, Tang R, Chai G and Jiang C 2018 *Appl. Phys. Lett.* **113** 042401
[32] Sang T, Zhang S, Zhao G, Geng C, Jin Z, Zong W, Cao D, Xu J, Wang X, Miao G X and Li S 2021 *J. Alloys Compd.* **875** 159881
[33] Ruderman M A and Kittel C 1954 *Phys. Rev.* **96** 99
[34] Kasuya T 1956 *Prog. Theor. Phys.* **16** 45
[35] Yosida K 1957 *Phys. Rev.* **106** 893